AIP | Applied Physics Letters

# Complete spectral gap in coupled dielectric waveguides embedded into metal

Wei Liu, Andrey A. Sukhorukov, Andrey E. Miroshnichenko, Chris G. Poulton, Zhiyong Xu, Dragomir N. Neshev, and Yuri S. Kivshar

Citation: Applied Physics Letters **97**, 021106 (2010); doi: 10.1063/1.3458694
View online: http://dx.doi.org/10.1063/1.3458694
View Table of Contents: http://scitation.aip.org/content/aip/journal/apl/97/2?ver=pdfcov
Published by the AIP Publishing

# Complete spectral gap in coupled dielectric waveguides embedded into metal

Wei Liu,[1,a)] Andrey A. Sukhorukov,[1] Andrey E. Miroshnichenko,[1] Chris G. Poulton,[2] Zhiyong Xu,[1] Dragomir N. Neshev,[1] and Yuri S. Kivshar[1]
[1]*Nonlinear Physics Center, Research School of Physics and Engineering, Australian National University, Canberra, ACT 0200, Australia*
[2]*Department of Mathematical Sciences, University of Technology, Sydney, New South Wales 2007, Australia*

(Received 3 May 2010; accepted 5 June 2010; published online 14 July 2010)

We study a plasmonic coupler involving backward ($TM_{01}$) and forward ($HE_{11}$) modes of dielectric waveguides embedded into an infinite metallic background. The simultaneously achievable contradirectional energy flows and codirectional phase velocities in different channels lead to a spectral gap, despite the absence of periodic structures along the waveguide. We demonstrate that a complete spectral gap can be achieved in a symmetric structure composed of four coupled waveguides. © *2010 American Institute of Physics*. [doi:10.1063/1.3458694]

Negative index metamaterials (NIMs) are artificial materials which have simultaneously negative permittivity and negative permeability.[1–4] In NIM waveguides, modes are *backward* when more energy flows in the NIM than in other channels. Coupling of a forward propagating mode in a conventional dielectric waveguide with a backward mode in a NIM waveguide has been investigated theoretically in both linear and nonlinear regimes.[4,5] The coupling of a forward mode and a backward one results in the formation of spectral gaps without periodic structures along the waveguide. This feedback mechanism may play an important role in nanophotonics, as it could significantly simplify complex geometries that are required for subwavelength optical manipulation and concentration. However, due to the fabrication complexity and high losses of NIM, coupling involving NIM is currently not experimentally feasible and therefore this mechanism has not attracted significant attention.

There has been a surging interest in the field of plasmonics, as it offers one of the most promising approaches for subwavelength optical concentration and manipulation (for a comprehensive review, see e.g., Refs. 6–9). In some plasmonic structures, backward modes exist in regimes when more energy flows in the metal than in the dielectric.[10–14] These structures are much simpler and more fabricable than those involving NIM. In this letter, we propose a design of plasmonic coupler involving the coupling between the backward $TM_{01}$ and the forward $HE_{11}$ modes in dielectric waveguides embedded into metal [see Fig. 1(a)]. We find a polarization dependent spectral gap in a structure of two coupled waveguides and a complete polarization independent gap in a $C_{3v}$ structure with four coupled waveguides.

It was recently reported[15] that taking experimental data of bulk metal[16] in numerical calculations of plasmonic modes may lead to losses which are much higher than real losses observed in experiments. In our study, we use the Drude model to simulate the optical properties of a metal as follows: $\varepsilon_m(\omega)=1-\omega_p^2/\omega(\omega+i\omega_\tau)$, where $\omega_p$ is the plasma frequency and $\omega_\tau$ is the collision frequency. At the same time, we define two normalized quantities as follows: loss $\gamma=\omega_\tau/\omega_p$ and size parameter $\alpha=\mathrm{R}\omega_p/\mathrm{c}$, where R is the radius of the dielectric core and c is speed of light in vacuum.

Figure 1(a) shows the two-waveguide structure we study; two dielectric rods of the same radius $\alpha=1.21$ (corresponding R is about 25nm for silver) with $\varepsilon_1=9$ and $\varepsilon_2=4$ are embedded into infinite metal. First, by analyzing the dispersion of a single waveguide, we find that the backward $TM_{01}$ mode for $\varepsilon=9$ intersects with the forward $HE_{11}$ mode for $\varepsilon=4$ at $\omega/\omega_p=0.3856$ [see Fig. 2(a)]. This point corresponds to $\lambda\approx 400$ nm for silver. For the $TM_{01}$ mode, more energy flows in the metal than in the dielectric, which is similar to the backward SPP on metallic wires.[10,17] It should be emphasized that the directionality of $TM_{01}$ and $HE_{11}$ modes are radius dependent as follows: the $TM_{01}$ mode can become forward when the radius increases and the $HE_{11}$ mode can become backward when the radius decreases.[12] However, the $HE_{11}$ mode has linear polarization inside the dielectric [see Fig. 2(c)], which could be excited directly with a normal incident wave,[18] whereas the $TM_{01}$ mode has radial polarization [see Fig. 2(d)] with much higher losses in the coupling region [see Fig. 2(b)].

Prior to preforming a fully numerical study, we use temporal coupled-mode theory[19,20] (TCMT) to get a qualitative understanding of dispersion relation in the lossless case. The eigenmodes of a coupled system are expressed as a superposition of individual waveguide modes as follows: $\mathbf{E}=\Sigma_m A_m(z,t)\mathbf{E}_m(x,y)e^{i(\omega_{m0}+\kappa_{mm})t}$, where $\omega_{m0}=\omega_m$ at $k=k_0$

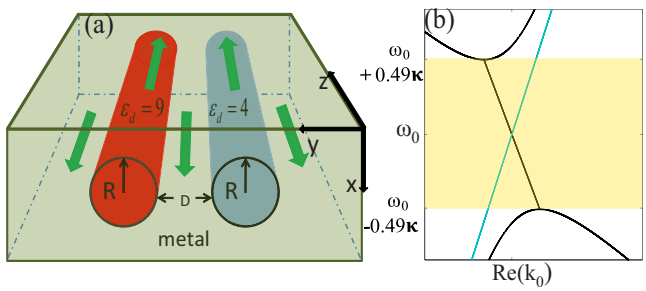


FIG. 1. (Color online) (a) Two dielectric waveduides with $\varepsilon_1=9$ and $\varepsilon_2=4$ separated by $D$ embedded into infinite metal. Arrows indicate the energy flow at different channels for the wave vector along $z$; (b) dispersion of two coupled waveguides. Shaded region indicates the incomplete polarization dependent spectral gap obtained using TCMT with $v_g=0.13\mathrm{c}$, $v_{g3}=-0.039\mathrm{c}$, and $\delta=0$.

a)Electronic mail: wli124@physics.anu.edu.au.

 

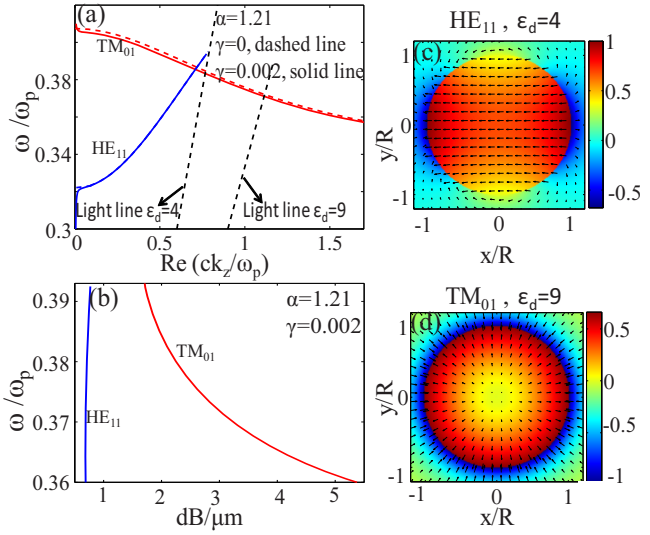


FIG. 2. (Color online) (a) Dispersion curve and (b) losses of $TM_{01}$ mode for $\varepsilon_d=9$ and $HE_{11}$ mode for $\varepsilon_d=4$. (c) and (d) Poynting vector component $S_z$ (colormap) and transverse electric field $E_t$ (arrows) for $HE_{11}$ mode and $TM_{01}$, respectively at $\omega/\omega_p=0.3856$ with $\gamma=0.002$.

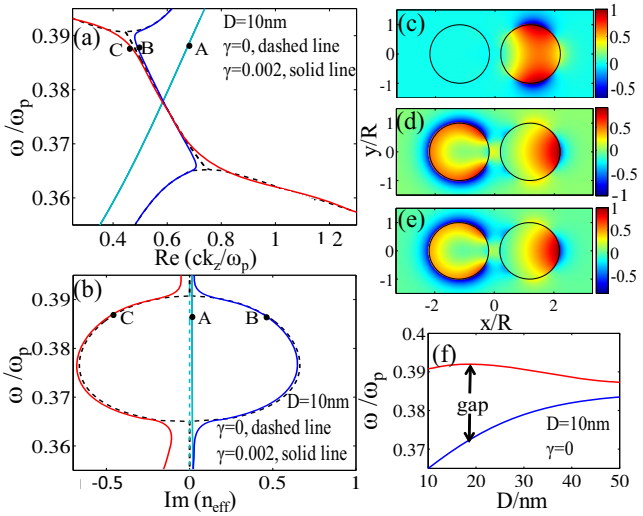


FIG. 3. (Color online) (a) Dispersion and (b) losses (imaginary part of $n_{\text{eff}}=k_z/k_0=k_z c/\omega$) of the three eigenmodes of the two-waveguide structure. Dashed black curves ($\gamma=0$) and solid curves with dots B and C ($\gamma=0.002$) correspond to modes of conjugated propagation constants. Dashed gray curve and solid curve with dot A (dashed curve almost overlaps the solid curve as the loss of this mode is comparatively low as shown in (b)] correspond to the $HE_{11}$ mode that is not coupled to the $TM_{01}$ mode as shown in (c). [(c)–(e)] $S_z$ of modes at the points A–C marked in (a) and (b), respectively. (f) Gap region vs distance between waveguides when $\gamma=0$.

and $\kappa_{mm}$ is the self-coupling coefficient. For the two coupled waveguides, three modes can couple to one another as follows: two forward $HE_{11}$ modes of preferred $x$ and $y$ polarizations, which could be approximately reconstructed by two orthogonal eigenmodes of circular polarizations $A_{1,2}(z,t)$ and one backward $TM_{01}$ mode $A_3(z,t)$. The coupled-mode equations in time domain are as follows:

$$i\frac{\partial A_{1,2}(z,t)}{\partial t}+iv_g\frac{\partial A_{1,2}(z,t)}{\partial z}+\kappa A_3(z,t)e^{i2\delta t}=0,$$

$$i\frac{\partial A_3(z,t)}{\partial t}+iv_{g3}\frac{\partial A_3(z,t)}{\partial z}+\kappa\sum_{m=1}^{2}A_m(z,t)e^{-i2\delta t}=0,$$

where $\delta=(1/2)(\kappa_{33}+\omega_{30}-\kappa_{11}-\omega_{10})=(1/2)(\kappa_{33}+\omega_{30}-\kappa_{22}-\omega_{20})$ is the antisymmetry parameter of two waveguides; $A_{1,2,3}$ are normalized envelopes; $v_{gi}(v_g=v_{g1,g2}>0, v_{g3}<0)$ are the group velocities at $\omega_0=\omega(k_0)$; $\kappa_{12}=\kappa_{21}=0$ (mode 1 and 2 are orthogonal); and the other mutual coupling coefficients are identical; $\kappa_{ij}=\kappa_{ji}=\kappa(i=1,2;j=3)$. In the coupling region we ignore the dispersion of group velocities and assume that $v_{g,g3}$ and $\kappa$ are constants. By introducing the following variables: $a_1(z,t)=A_1(z,t)e^{-i\delta t}$, $a_2(z,t)=A_2(z,t)e^{-i\delta t}$, and $a_3(z,t)=A_3(z,t)e^{i\delta t}$, and applying the Fourier transform, we obtain the propagation constants of three eigenmodes: $k_{1,2}=(\alpha\pm i\sqrt{-8v_{g3}v_g\kappa^2-\beta^2})/2v_gv_{g3}$, $k_3=(\omega+\delta)/v_g$ where $\alpha=v_g(\omega-\delta)+v_{g3}(\omega+\delta)$ and $\beta=v_g(\omega-\delta)-v_{g3}(\omega+\delta)$. When $-8v_{g3}v_g\kappa^2\geq\beta^2$, $k_{1,2}$ is a conjugated pair, indicating the existence of a spectral gap, while $k_3$ corresponds to the eigenmode $\hat{a}(k,\omega)=\hat{a}_1(k,\omega)+\hat{a}_2(k,\omega)$, where $\hat{a}_1(k,\omega)$ and $\hat{a}_2(k,\omega)$ denote orthogonal circularly polarized modes. Thus, $k_3$ corresponds to a linearly polarized $HE_{11}$ mode, which is not coupled to the $TM_{01}$ mode. This mode makes the gap dependent on the polarization. Figure 1(b) shows the results obtained using TCMT of $\delta=0$ when values with $v_{g,g3}$ are taken from Fig. 2(a).

Full numerical simulation results using COMSOL (see Fig. 3) qualitatively agree with TCMT. In the lossless case $\gamma=0$, the spectral gap is defined by a pair of complex conjugated propagation constants [see Figs. 3(a) and 3(b)]. The gap width increases with decreasing the distance $D$ [see Fig. 3(f)], because the coupling coefficient becomes larger. When we incorporate some losses ($\gamma=0.002$), all modes become complex and the definition of width of the gap depends on how far it is from the observing point to the source. However, the gap width of lossless metal ($\gamma=0$) may still serve as a guide and effective approximation as shown in Figs. 3(a) and 3(b). In addition to the modes of conjugated propagation constants, there exists one more $HE_{11}$ like decoupled mode. The energy flow of this mode is mostly confined inside $\varepsilon_1=4$ waveguide [see Fig. 3(c)]. Thus, the gap of the two coupled waveguides is incomplete and polarization dependent.

To make modes of different preferred polarization directions degenerate and obtain a full gap, symmetric structures could be used.[21,22] One of the options is to utilize four-waveguide $C_{3v}$ structure [see Fig. 4(a)]. We use subscripts $n=1,2$ to denote two $HE_{11}$ modes of circular polarizations and $n=3,4,5$ for three $TM_{01}$ modes. Based on the symmetry and energy conservation law in the lossless case, the following relations are satisfied for mutual coupling coefficients: $\kappa_{12}=\kappa_{21}=0$, $\kappa_{1m}=\kappa_{m1}^*=\kappa_{2m}^*=\kappa_{m2}=\kappa_1 e^{2/3\pi(m-3)i}$ for $m,n=3,4,5$ and $m\neq n$. Due to the $C_{3v}$ symmetry, eigenmodes $\hat{a}(k,\omega)=\Sigma_{m=1}^{5}\beta_m\hat{a}_m(k,\omega)$ of preferred $x$ polarization ($\beta_1=\beta_2$) and those of preferred $y$ polarization ($\beta_1=-\beta_2$) should be degenerate.[21,22] Thus using TCMT we can find five eigenmodes of three frequencies: $k_{1,2}=(\alpha\pm i\sqrt{-12v_{g3}v_g\kappa^2-\beta^2})/2v_gv_{g3}$ (corresponding to two degenerate pairs of modes), $\omega=\omega_3(k)+2\kappa_2$, where $\alpha=v_g(\omega-\delta+\kappa_2)+v_{g3}(\omega+\delta)$, $\beta=v_g(\omega-\delta+\kappa_2)-v_{g3}(\omega+\delta)$ and $\omega_3(k)$ is the dispersion of the individual $TM_{01}$ mode. Again $k_{1,2}$ can be a conjugated pair, indicating the existence of a gap. $\omega=\omega_3(k)+2\kappa_2$ corresponds to eigenmode (E3 mode) $\hat{a}(k,\omega)=\Sigma_{m=3}^{5}\hat{a}_m(k,\omega)$, which is a symmetric combination of $TM_{01}$ modes. The cut-off frequency of E3 mode is shifted by

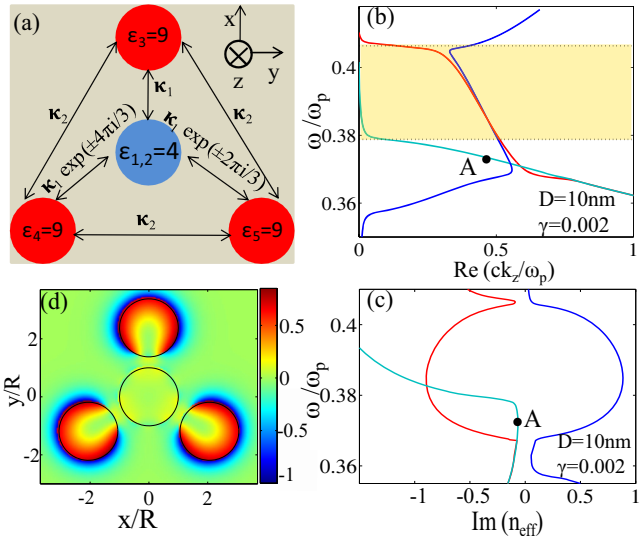


FIG. 4. (Color online) (a) Schematic of the four-waveguide structure with $C_{3v}$ symmetry. The distance between $\varepsilon_{1,2}$ waveguide to $\varepsilon_{3,4,5}$ waveguides is D. (b) Dispersion and (c) losses of three eigenmodes. Curves with dot A correspond to the E3 mode. The complete gap region in lossless case is shaded. (d) $S_z$ of E3 mode at point A marked in (b) and (c).

$2\kappa_2$ compared with individual $TM_{01}$ mode. Numerical results from COMSOL are shown in Fig. 4. This allows us to conclude that the spectral gap indicated by the yellow region of four coupled waveguides becomes polarization independent when the E3 mode is cutoff. For larger losses (metal in deep ultraviolet regime) the spectral gap still exists but the effective width becomes smaller and eventually disappears as increasing losses make the differences between gap and nongap region smaller. To enable coupling at longer-wavelength regimes, where losses of metal are lower, one could use dielectric waveguides with higher permittivities (GaAs, for example).

In summary, we have studied a coupler based on two dielectric waveguides in metal involving the coupling of backward and forward waves. By using the TCMT we have predicted a spectral gap in such a system without a periodic structure. This result has been verified by direct numerical simulations. Moreover, we have demonstrated that a complete polarization independent gap can be achieved by using four coupled waveguides with $C_{3v}$ symmetry. Similar coupling between surface plasmon polaritons (SPPs) can happen in metallic-wire structures when the radius is small enough to support backward SPPs.[10] However, high losses of backward SPPs on metallic wires prevent them from realistic realizations. We anticipate that by incorporating materials with gain and/or nonlinearities, the proposed structure can be considered as a platform for the study of gap solitons, optical bistability, high-Q cavities, and plasmonic nanolaser in various systems without periodicity.

The authors acknowledge a financial support from the Australian Research Council and useful discussions with B. T. Kuhlmey, I. V. Shadrivov, A. R. Davoyan, T. P. White, D. A. Powell, R. Iliew, A. S. Solntsev, and J. F. Zhang.

[1]V. G. Veselago, Sov. Phys. Usp. **10**, 509 (1968).
[2]R. A. Shelby, D. R. Smith, and S. Schultz, Science **292**, 77 (2001).
[3]G. V. Eleftheriades and K. G. Balmain, *Negative Refraction Metamaterials: Fundamental Principles and Applications* (Wiley, New York, 2005).
[4]A. Alu and N. Engheta, in *Negative-Refraction Metamaterials*, edited by G. V. Eleftheriades and K. G. Balmain (Wiley, New York, 2005).
[5]N. M. Litchinitser, I. R. Gabitov, and A. I. Maimistov, Phys. Rev. Lett. **99**, 113902 (2007).
[6]W. L. Barnes, A. Dereux, and T. W. Ebbesen, Nature (London) **424**, 824 (2003).
[7]S. A. Maier, *Plasmonics: Fundamentals and Applications* (Springer, Berlin, 2007).
[8]D. K. Gramotnev and S. I. Bozhevolnyi, Nat. Photonics **4**, 83 (2010).
[9]J. A. Schuller, E. S. Barnard, W. Cai, Y. C. Jun, J. S. White, and M. L. Brongersma, Nature Mater. **9**, 193 (2010).
[10]C. A. Pfeiffer, E. N. Economou, and K. L. Ngai, Phys. Rev. B **10**, 3038 (1974).
[11]J. J. Burke, G. I. Stegeman, and T. Tamir, Phys. Rev. B **33**, 5186 (1986).
[12]B. Prade and J. Y. Vinet, J. Lightwave Technol. **12**, 6 (1994).
[13]L. Novotny and C. Hafner, Phys. Rev. E **50**, 4094 (1994).
[14]M. Wegener, G. Dolling, and S. Linden, Nature Mater. **6**, 475 (2007).
[15]Y. Ma, X. Li, H. Yu, L. Tong, Y. Gu, and Q. Gong, Opt. Lett. **35**, 1160 (2010).
[16]P. B. Johnson and R. W. Christy, Phys. Rev. B **6**, 4370 (1972).
[17]H. Khosravi, D. R. Tilley, and R. Loudon, J. Opt. Soc. Am. A **8**, 112 (1991).
[18]H. Shin, P. B. Catrysse, and S. Fan, Phys. Rev. B **72**, 085436 (2005).
[19]G. P. Agrawal, *Nonlinear Fiber Optics* (Elsevier, San Diego, 2007).
[20]C. M. de Sterke, D. G. Salinas, and J. E. Sipe, Phys. Rev. E **54**, 1969 (1996).
[21]P. R. McIsaac, IEEE Trans. Microwave Theory Tech. **23**, 421 (1975).
[22]M. J. Steel T. P. White C. M. de. Sterke, R. C. McPhedran, and L. C. Botten, Opt. Lett. **26**, 488 (2001).